CHAPTER VIII

Effect of Thermal Radiation and Chemical Reaction on Three Dimensional MHD Fluid Flow in a Porous Medium – A Numerical Study

8.1. Introduction

The study of radiation effect on magnetic flow plays a vital role in many industries such as Nuclear power plants, Aircrafts, Gas turbines, space vehicles, etc., The radiation effect is quite significant at high operating temperature. Many engineering processes occur at high temperature and knowledge of radiation heat transfer becomes very important. Effect of chemical reaction also occurs in many branches of science and engineering. Chemical processes have numerous industrial applications such as manufacturing of glassware, food processing, filtration and purification process in chemical engineering, etc., In particular, the study of chemical reaction with heat radiation is of considerable importance in chemical and hydrometallurgical industries.

Cortell (2008) studied the flow of viscous fluid over a nonlinearly stretching surface in the presence of viscous dissipation and radiation effects. Hossain and Takhar (1996) studied radiation effects on mixed convection along an isothermal vertical plate. The effect of thermal radiation on free convective flow past a moving vertical plate was discussed by Raptis and Perdikis (1999). The thermal radiation effects on flow past an impulsively started infinite vertical plate in the presence of magnetic field was studied by Muthucumaraswamy and Janakiraman (2006). Pop *et al*. (2004) analyzed the radiation effects on the flow near the stagnation point of a stretching sheet. Effect of thermal radiation on heat and mass transfer flow near the stagnation point towards a stretching sheet in porous medium was carried out by Salem and Fathy (2012). Steady two-dimensional magnetic flow of a viscous incompressible electrically conducting fluid in the presence of radiation effect was studied by Phool Singh *et al*. (2011).

Krishnendu Bhattacharyya *et al*. (2012) studied the effect of chemical reaction on boundary layer stagnation-point of an electrically conducting fluid in the presence of a magnetic field using quasilinearization technique. Three dimensional free convective flow with heat and mass transfer through a porous medium in the presence of magnetic field and chemical reaction using perturbation method was studied by

Pravat Kumar Rath *et al*. (2013). Sarma and Mahanta (2015) studied the effect of chemical reaction on three-dimensional mass transfer flow in the presence of a magnetic field using perturbation technique.

Ahmed and Kalita (2013) analyzed the two-dimensional non-linear heat and mass transfer of an incompressible, viscous, electrically conducting fluid in the presence of magnetic field, chemical reaction of first order and thermal radiation effects. The effect of thermal radiation and chemical reaction on two-dimensional magnetic field with heat and mass transfer was discussed by Kartikeyan *et al*. (2016). The effect of radiation and chemical reaction on a two-dimensional steady magnetic field with mixed convective flow of heat and mass transfer was studied by Singh (2011). Steady three-dimensional flow for an incompressible, viscous fluid past a stretching sheet using the homotopy perturbation method was studied by Donald Ariel (2007).

The above mentioned studies have ignored the effect of magnetic field and porosity on three-dimensional steady flow. This gap motivates us to take up the present work wherein we study the effect of magnetic field on three-dimensional steady flow along with heat and mass transfer over a porous plate embedded in a porous medium. In order to examine the accuracy of our result, the effect of stretching ratio on velocities $f'(\eta), g'(\eta)$ are calculated and plotted. The results obtained are validated for vanishing chemical reaction, thermal radiation, magnetic field and porosity parameter which were found to be in good agreement with the results obtained by Donald Ariel (2007). In the present work, temperature and mass concentration are also taken into an account.

8.2. Flow Description and Governing Equations

We consider a steady three dimensional laminar flow of an incompressible viscous electrically conducting fluid induced by the stretching of the flat surface in two lateral directions in an otherwise quiescent fluid. At the same time, the wall temperature is raised from T_∞ to T_w $(T_w > T_\infty)$ and the concentration is raised from C_∞ to C_w $(C_w > C_\infty)$.The magnetic field is applied in the z-direction. We can neglect the effect of the induced magnetic field in comparison to the applied magnetic field. The electrical current flowing in the fluid gives rise to an induced magnetic field if the fluid were an electrical insulator, but here we have taken the fluid to be electrically conducting.

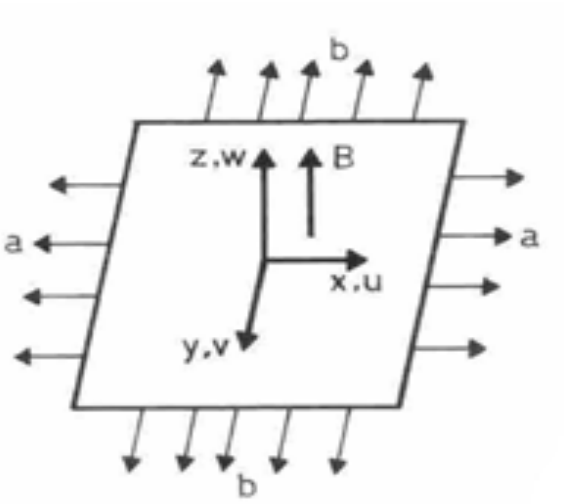

Fig 8.1 Physical Configuration of the problem

In the present work, the following assumptions are made:

- Flow of a Newtonian and electrically conducting fluid is considered which is three dimensional, steady, viscous, incompressible electrically conducting and laminar in nature.
- Fluid is induced by the stretching of the flat surface in two lateral directions in an otherwise quiescent fluid.
- Magnetic field is applied in the z-direction.
- The effect of the induced magnetic field is neglected in comparison to the applied magnetic field.
- Radiation and chemical reaction effects are separately considered in the present problem.
- The wall temperature is raised from T_∞ to T_w $(T_w > T_\infty)$.
- The concentration is raised from C_∞ to C_w $(C_w > C_\infty)$.

Under these assumptions, the governing equations for the continuity, momentum and energy can be written as follows:

$$\frac{\partial u}{\partial x} + \frac{\partial v}{\partial y} + \frac{\partial w}{\partial z} = 0 \tag{8.1}$$

$$u\frac{\partial u}{\partial x} + v\frac{\partial u}{\partial y} + w\frac{\partial u}{\partial z} = \gamma\frac{\partial^2 u}{\partial z^2} - \frac{\sigma B_0^2}{\rho}u - \frac{\gamma}{k}u \tag{8.2}$$

$$u\frac{\partial v}{\partial x} + v\frac{\partial v}{\partial y} + w\frac{\partial v}{\partial z} = \gamma\frac{\partial^2 v}{\partial z^2} - \frac{\sigma B_0^2}{\rho}v - \frac{\gamma}{k}v \tag{8.3}$$

$$u\frac{\partial T}{\partial x} + v\frac{\partial T}{\partial y} + w\frac{\partial T}{\partial z} = \frac{\kappa}{\rho C_p}\frac{\partial^2 T}{\partial z^2} + \frac{16\sigma T_\infty^3}{3\rho C_p k_1}\left(\frac{\partial^2 T}{\partial z^2}\right) \tag{8.4}$$

$$u\frac{\partial C}{\partial x} + v\frac{\partial C}{\partial y} + w\frac{\partial C}{\partial z} = D_M\frac{\partial^2 C}{\partial z^2} + D_T\frac{\partial^2 T}{\partial z^2} - k_0(C - C_\infty) \tag{8.5}$$

where T, C, μ, σ and $\gamma = (\mu/\rho)$ represent respectively the temperature, mass concentration, coefficient of viscosity, electrical conductivity and the kinematic viscosity of the fluid. The constant parameters in the system: $k, C_p, \kappa,\ D_M$ and D_T represent respectively the permeability of porous material, specific heat at constant pressure, thermal conductivity of the fluid, molecular diffusivity and thermal diffusivity.

The appropriate boundary conditions are given by,

$$u = u_w(x) = ax\ , v = v_w(y) = by,\ w = 0,\ T = T_w(x)\ , C = C_w(x) \text{ at } z = 0 \tag{8.6}$$

$$u \to 0,\ v \to 0,\ w \to 0, T \to T_\infty\ ,\ C \to C_\infty \text{ as } z \to \infty \tag{8.7}$$

8.3. Solution of the Problem

We use similarity technique to solve the system of equations (8.1)-(8.5) along with the boundary conditions (8.6) and (8.7). The similarity transformations are,

$$\eta = \sqrt{\frac{a}{\gamma}}\, z\ , u = axf'(\eta), v = byg'(\eta),$$

$$w = -\sqrt{a\gamma}\,[f(\eta) + cg(\eta)], \theta(\eta) = \frac{T - T_\infty}{T_w - T_\infty}, \phi(\eta) = \frac{C - C_\infty}{C_w - C_\infty} \tag{8.8}$$

where $c = b/a$ is the stretching ratio of the velocities in y and x- directions, and prime denote differentiation with respect to η. Making use of (8.6) and (8.7), equation of continuity is identically satisfied and introducing the above transformations in equations (8.2)-(8.5) along with boundary conditions (8.6) and (8.7), we obtain the system of ordinary differential equations,

$$f''' + (f + cg)f'' - f'^2 - (M + k^*)f' = 0, \tag{8.9}$$

$$g''' + (f + cg)g'' - cg'^2 - (M + k^*)g' = 0, \tag{8.10}$$

$$\left(1 + \frac{4}{3}N\right)\theta'' + (Prf + Prcg)\theta' = 0, \tag{8.11}$$

$$\phi'' + (Scf + Sccg)\phi' + ScSr\theta'' - Sc\beta\phi = 0. \tag{8.12}$$

The transformed boundary conditions are given as,

$$f(\eta) = 0,\ f'(\eta) = 1,\ g(\eta) = 0,\ g'(\eta) = c, \theta(\eta) = 1,\ \phi(\eta) = 1 \text{ at } \eta = 0; \tag{8.13}$$

$$f'(\eta) \to 0,\ g'(\eta) \to 0, \theta(\eta) \to 0,\ \phi(\eta) \to 0 \text{ as } \eta \to \infty \tag{8.14}$$

where $M = \frac{\sigma B_0^2}{a\rho}$ is the magnetic parameter, $Pr = \mu C_p/\kappa$ is the Prandtl number, $Sc = \frac{\gamma}{D_m}$ is the Schmidt number, $Sr = \frac{(T_w - T_\infty)D_T}{(C_w - C_\infty)\gamma}$ is the Soret number, $k^* = \gamma/ka$ is

the permeability of porous medium, $Re_x = \frac{ax^2}{\gamma}$ is the Reynolds number, $N = \frac{4\sigma T_\infty^3}{kk_1}$ is the radiation parameter and $\beta = \frac{k_0}{a}$ is the reaction rate parameter.

The non-linear coupled ordinary differential equations (8.9)-(8.12) subject to boundary conditions (8.13)-(8.14) are reduced to a system of first order ordinary differential equations as follows,

$f' = w,\ w' = v, g' = a,\ a' = A, \theta = y,\ \theta' = z,\ \phi = b,\ \phi' = e$

$$v' = -(x + ci)v + w^2 + (M + k^*)w \tag{8.15}$$

$$A' = -(x + ci)A + ca^2 + (M + k^*)a \tag{8.16}$$

$$z' = -\frac{1}{\left(1+\frac{4}{3}N\right)}(Prx + Prci)z, \tag{8.17}$$

$$e' = -(Scx + Scci)e + \left(\frac{1}{\left(1+\frac{4}{3}N\right)}\right)(ScSrPrx + ScSrPrci)z + Sc\beta b \tag{8.18}$$

and boundary conditions become,

$$x(0) = 0,\ \ w(0) = 1, i(0) = 0, a(0) = 1, y(0) = 1,\ b(0) = 1 \ \text{ at } \eta = 0 \tag{8.19}$$

$$w(0) \to 0, a(0) \to 0, y(0) \to 0,\ b(0) \to 0 \quad \text{as } \eta \to \infty \tag{8.20}$$

We have solved the equations (8.15)-(8.18) with boundary conditions (8.19) and (8.20) using shooting method.

The major physical quantities - the skin-friction coefficient C_f, the local Nusselt number Nu_x, and local Sherwood number Sh_x are defined respectively as follows,

Expressions for skin-friction coefficient C_f on the surface along x and y directions, denoted by C_{fx} and C_{fy} respectively are as follows:

$$C_{fx} = \frac{\tau_{wx}}{\rho u_w^2}, C_{fy} = \frac{\tau_{wy}}{\rho u_w^2}$$

where τ_{wx} and τ_{wy} are the shear stress along x and y directions respectively.

Local Nusselt number: $Nu_x = \frac{xq_w}{k(T_w - T_\infty)}$

Local Sherwood number: $Sh_x = \frac{xq_m}{D(C_w - C_\infty)}$

where q_w is the heat flux, q_m is the mass flux at the surface respectively.

$\tau_{wx} = \mu\left(\frac{\partial u}{\partial z}\right)_{z=0}, \tau_{wy} = \mu\left(\frac{\partial v}{\partial z}\right)_{z=0}, \ q_w = -k\left(\frac{\partial T}{\partial z}\right)_{z=0}, q_m = -D\left(\frac{\partial C}{\partial z}\right)_{z=0}$

Applying the non-dimensional transformations (8.8) we obtain,

$$f''(0) = C_{fx}(Re_x)^{1/2}$$

$$cg''(0) = \left(\frac{x}{y}\right) C_{fy}(Re_x)^{1/2}$$

$$-\theta'(0) = Nu_x(Re_x)^{-1/2}$$

$$-\phi'(0) = xSh_x(Re_x)^{-1/2}$$

where $Re_x = \frac{xu_x(x)}{\gamma}$ is the local Reynolds number based on the stretching velocity $u_x(x)$.

8.4. Results and Discussion

In order to get the physical insight of the problem we have studied the velocity profiles $f'(\eta), g'(\eta)$, temperature profile $\theta(\eta)$ and concentration profile $\phi(\eta)$ against various parameters such as magnetic field M, stretching ratio c, Schmidt number Sc, Soret number Sr, porosity parameter k^*, thermal radiation N and chemical reaction β. The effect of various flow parameters on velocity field, skin-friction, Nusselt number and Sherwood number are calculated numerically and discussed with the help of graphs.

To check the validity of the expressions derived in the previous section we have shown the effect of stretching ratio on velocities through figures (8.2) and (8.3) for vanishing chemical reaction, thermal radiation, magnetic field and porosity parameter. It can be seen from these figures that the increase in stretching ratio decreases the main flow velocity $f'(\eta)$ and increases the cross flow velocity $g'(\eta)$. These results are in agreement with Donald Ariel (2007).

Figures (8.4)-(8.7) represent the effect of magnetic parameter M on velocity profiles $f'(\eta), g'(\eta)$, temperature profile $\theta(\eta)$ and concentration profile $\phi(\eta)$. It is observed that the increase in magnetic parameter M causes decrease in velocity profiles $f'(\eta), g'(\eta)$ and increase in temperature $\theta(\eta)$ and concentration $\phi(\eta)$ profiles. It is evident that an increase in the magnetic parameter retards the flow and enhances the temperature and concentration profiles. It is due to the fact that the increasing magnetic field parameter improves the opposite force to the flow of direction which is called Lorentz force. From this we observe that the Lorentz force slows down the motion of electrically conducting fluids.

Figures (8.8) - (8.11) represent the effect of stretching ratio parameter c on velocity profiles $f'(\eta), g'(\eta)$, temperature profile $\theta(\eta)$ and concentration profile $\phi(\eta)$. It is clear that an increase in stretching ratio decreases main flow velocity

$f'(\eta)$, temperature $\theta(\eta)$ and concentration $\phi(\eta)$ profiles and increases cross flow velocity profile $g'(\eta)$.

Figures (8.12) and (8.13) exhibit the effect of Schmidt number Sc and Soret number Sr on concentration profiles. These two figures illustrate that the increase in Schmidt number Sc and Soret number Sr causes the decrease and increase in concentration profiles respectively.

Figures (8.14) and (8.15) exhibit the effect of porosity parameter k^* on velocity profiles $f'(\eta)$ and $g'(\eta)$. It is evident from these figures that an increase in porosity parameter k^* decreases main and cross flow velocities $f'(\eta)$ and $g'(\eta)$.

Figure (8.16) shows the effect of radiation parameter N on temperature profile $\theta(\eta)$. It is observed that increase in the radiation parameter enhances the temperature profile. This is because of heat release from the energy of the flow due to a rise in the radiation parameter.

Figure (8.17) shows the effect of chemical reaction parameter β on concentration profile $\phi(\eta)$. It is clear that increase in the chemical reaction parameter decreases the concentration profile.

Table (8.I) illustrates the variation in skin-friction coefficient, local Nusselt number and local Sherwood number for different values of non-dimensional parameters such as magnetic parameter M, stretching ratio c, radiation parameter N, chemical reaction parameter β. It shows that magnetic parameter M has a tendency to reduce the skin-friction factor and increase the rate of heat and mass transfer. Radiation parameter enhances the rate of heat transfer and decreases the rate of mass transfer slightly. Due to increase in chemical reaction parameter, rate of mass transfer decreases. It is clear that stretching ratio reduces skin-friction and rate of heat transfer, and increases the rate of mass transfer.

8.5. Conclusion

The influence of thermal radiation and chemical reaction on steady three-dimensional free-convective incompressible viscous electrically conducting fluid flow with heat and mass transfer over a porous flat plate in the presence of magnetic field embedded in porous medium is investigated. The non-linear boundary layer equations together with the boundary conditions are reduced to a system of non-linear ordinary differential equations by using similarity transformations. The system of non-linear

ordinary differential equations is solved by shooting procedure using fourth order Runge-Kutta Method.

From the present study, we conclude that an increase in radiation parameter N causes an increase in temperature $\theta(\eta)$ profile and an increase in chemical parameter β causes decrease in concentration $\phi(\eta)$ profile. Skin-friction coefficient, local Nusselt number and local Sherwood number are discussed for different values of non-dimensional parameters.

In this study the following conclusions are set out:

- Magnetic parameter reduces skin-friction and increase the rate of heat and mass transfer.
- Radiation parameter enhances the rate of heat transfer and decrease the rate of mass transfer.
- Increase in chemical reaction parameter decreases the rate of mass transfer.
- Increase in stretching ratio reduces skin-friction and rate of heat transfer.
- Due to increase in stretching ratio rate of mass transfer increases.

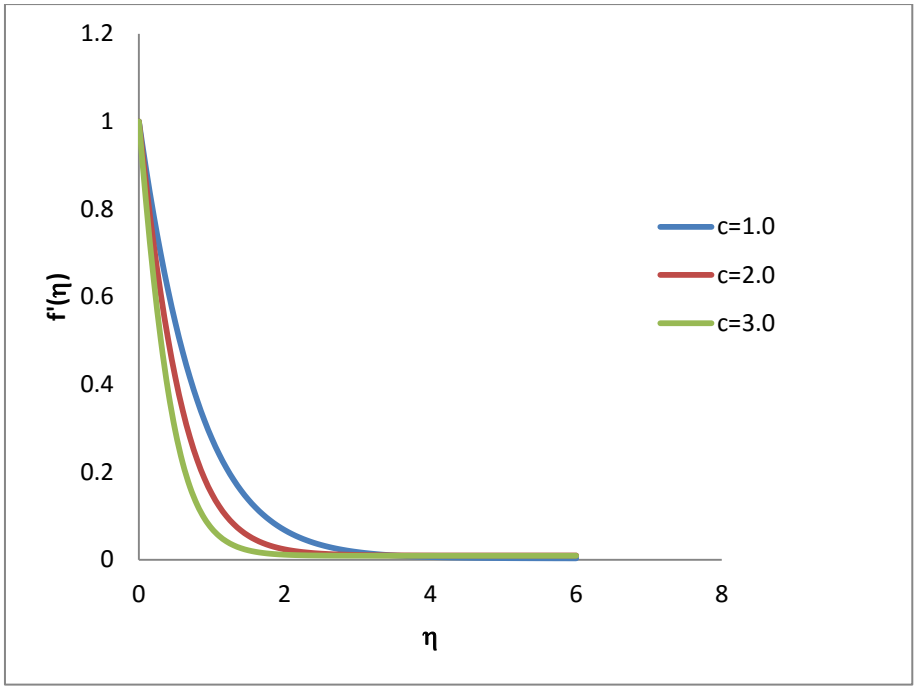

Fig 8.2 Effect of stretching ratio on velocity $f'(\eta)$.
When $N = \beta = M = k^* = 0$

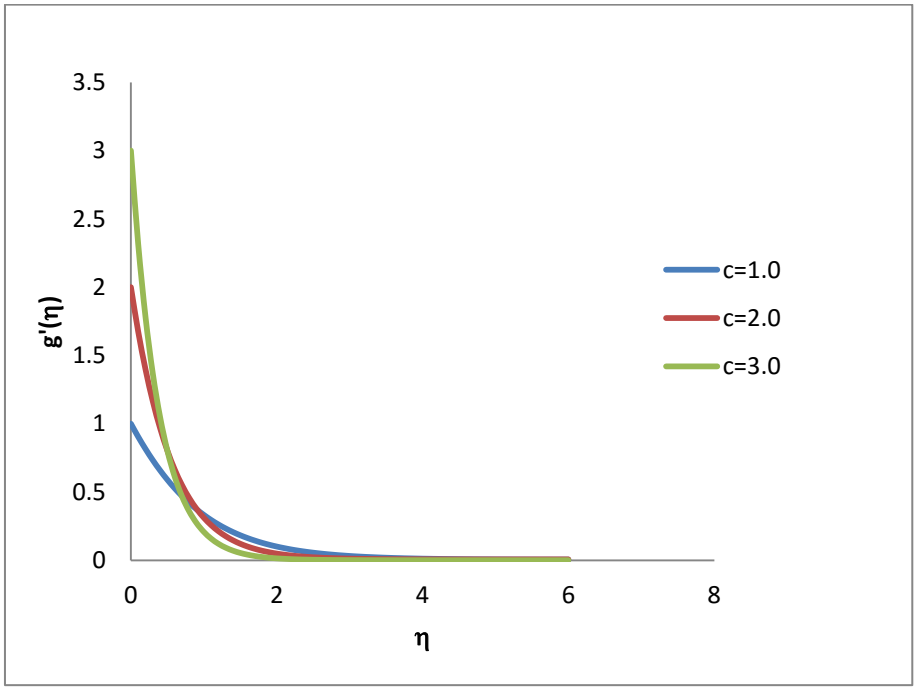

Fig 8.3 Effect of stretching ratio on velocity $g'(\eta)$.
When $N = \beta = M = k^* = 0$

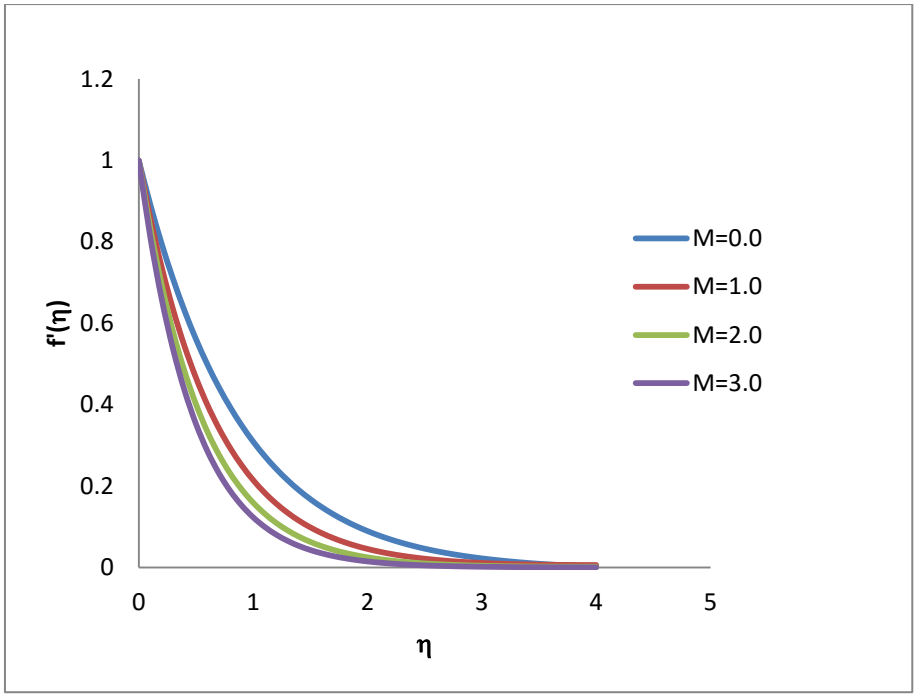

Fig 8.4 Effect of magnetic parameter M on velocity $f'(\eta)$; Pr=7.0; k=0.2; Sc=0.3; Sr=0.3; c= 0.5; N=0.5; β=0.5*

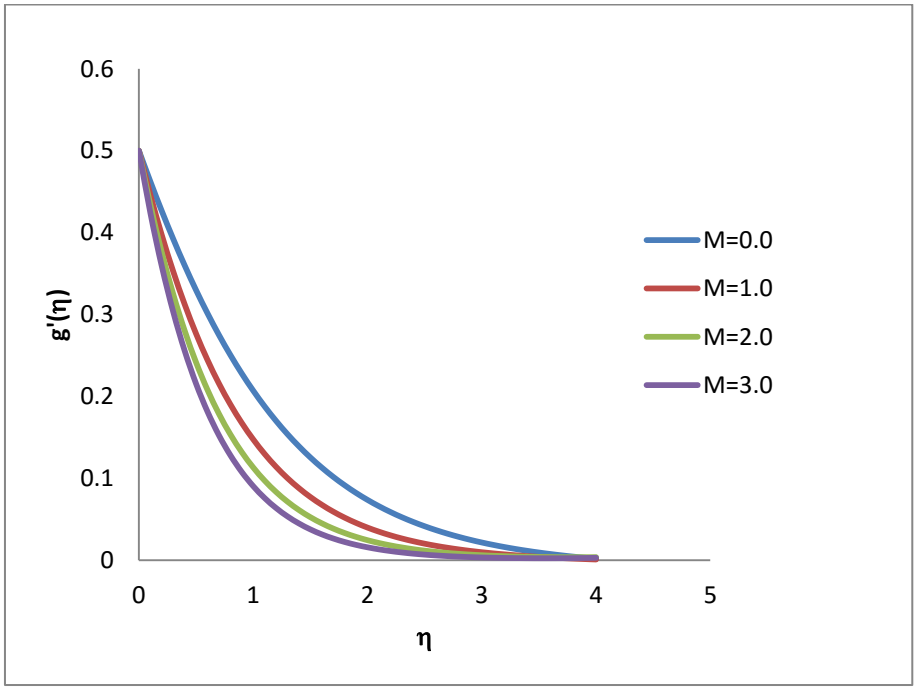

Fig 8.5 Effect of magnetic parameter M on velocity $g'(\eta)$; Pr=7.0; k=0.2; Sc=0.3; Sr=0.3; c= 0.5; N=0.5; β=0.5*

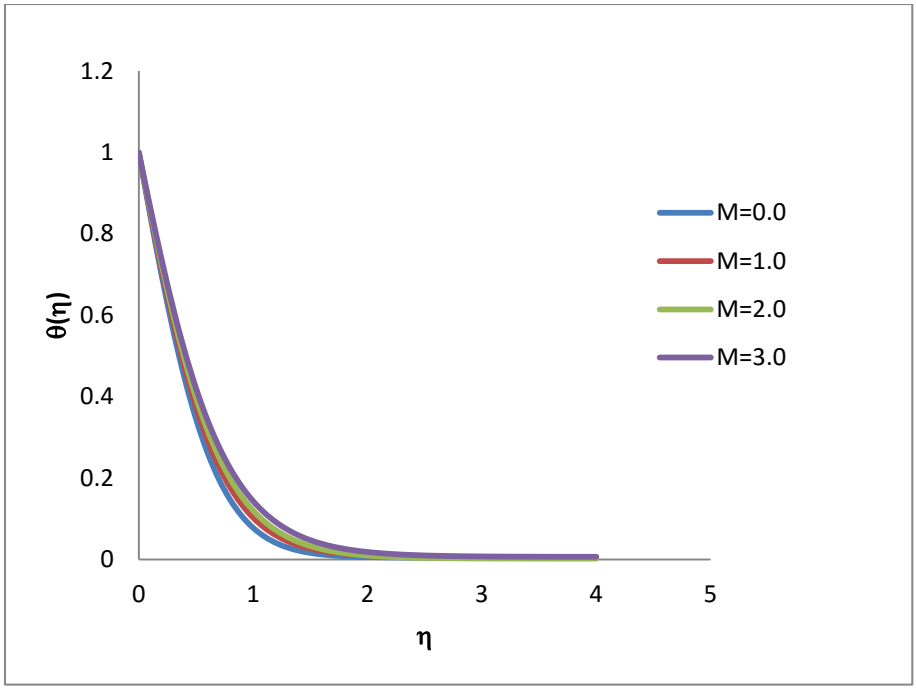

Fig 8.6 Effect of magnetic parameter M on temperature $\theta(\eta)$; Pr=7.0; k=0.2; Sc=0.3; Sr=0.3; c= 0.5; N=0.5; β=0.5*

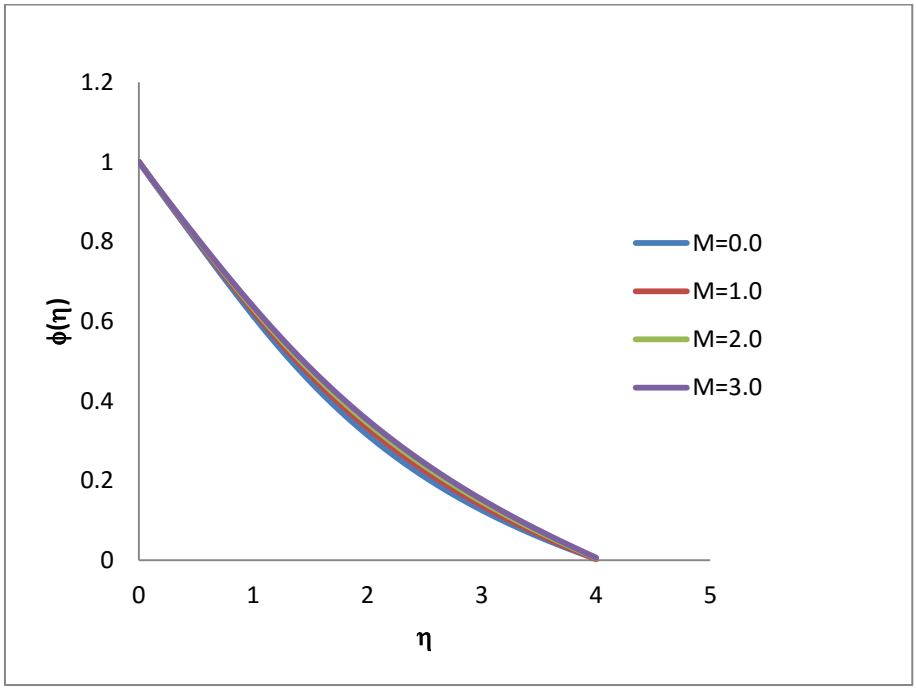

Fig 8.7 Effect of magnetic parameter M on concentration $\phi(\eta)$; Pr=7.0; k=0.2; Sc=0.3; Sr=0.3; c= 0.5; N=0.5; β=0.5*

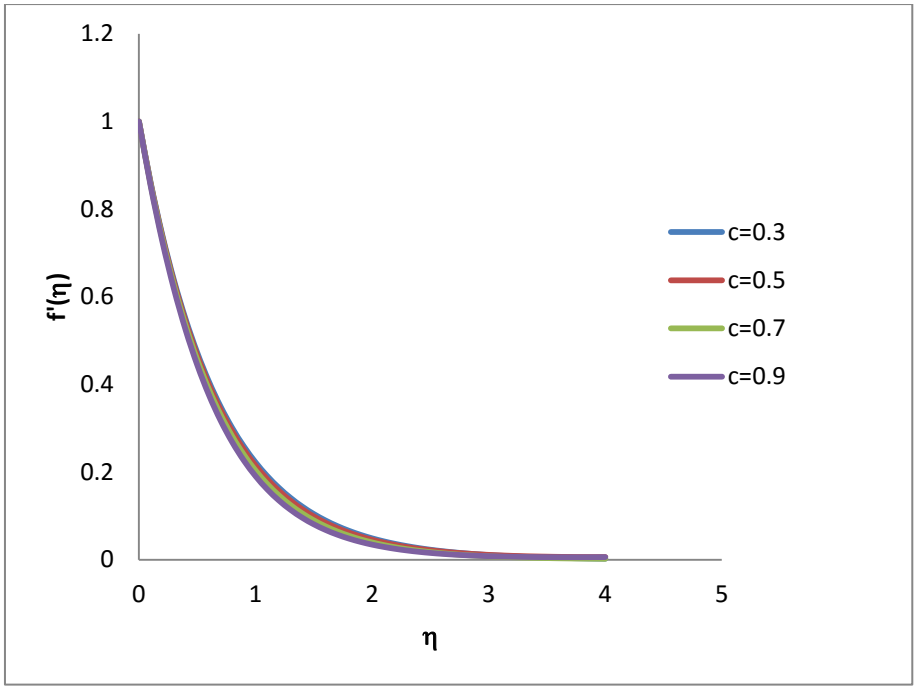

Fig 8.8 Effect of stretching ratio c on velocity $f'(\eta)$; Pr=7.0; k=0.2; Sc=0.3; Sr=0.3; M = 1.0; N=0.5; β=0.5*

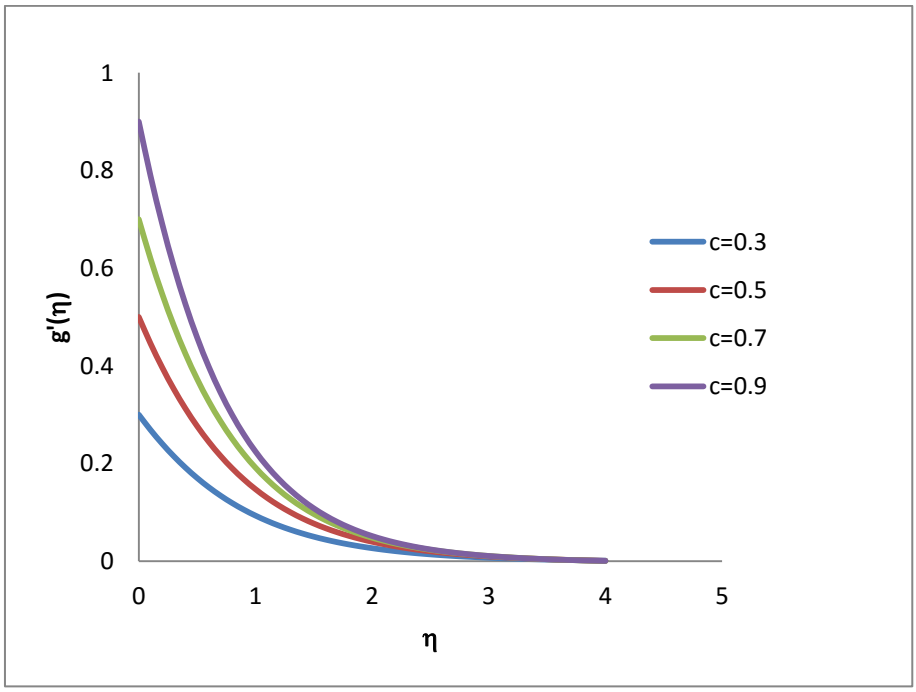

Fig 8.9 Effect of stretching ratio c on velocity $g'(\eta)$; Pr=7.0; k=0.2; Sc=0.3; Sr=0.3; M = 1.0; N=0.5; β=0.5*

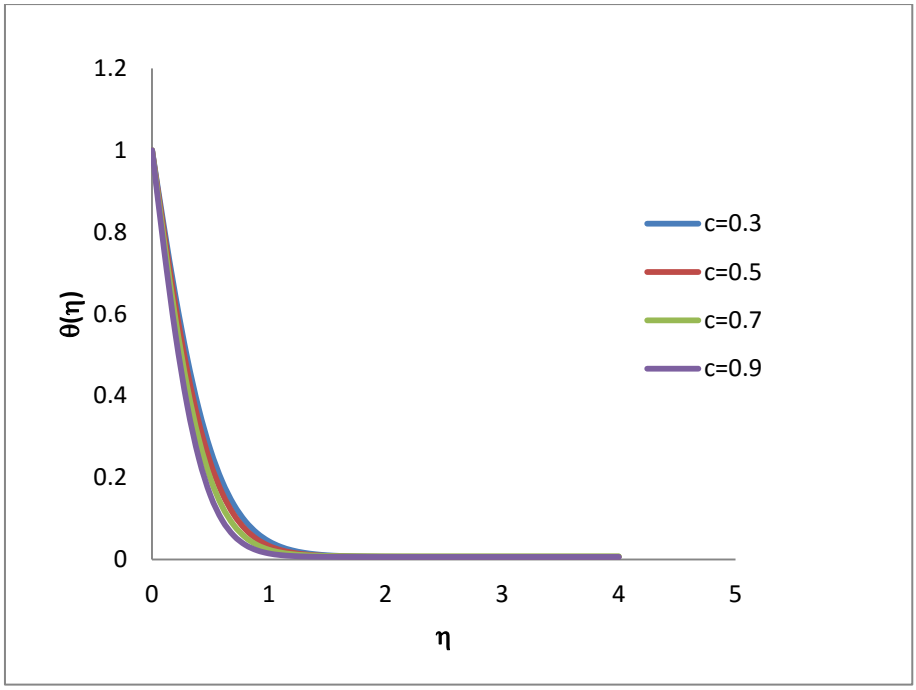

Fig 8.10 Effect of stretching ratio c on temperature $\theta(\eta)$; Pr=7.0; k=0.2; Sc=0.3; Sr=0.3; M = 1.0; N=0.5; β=0.5*

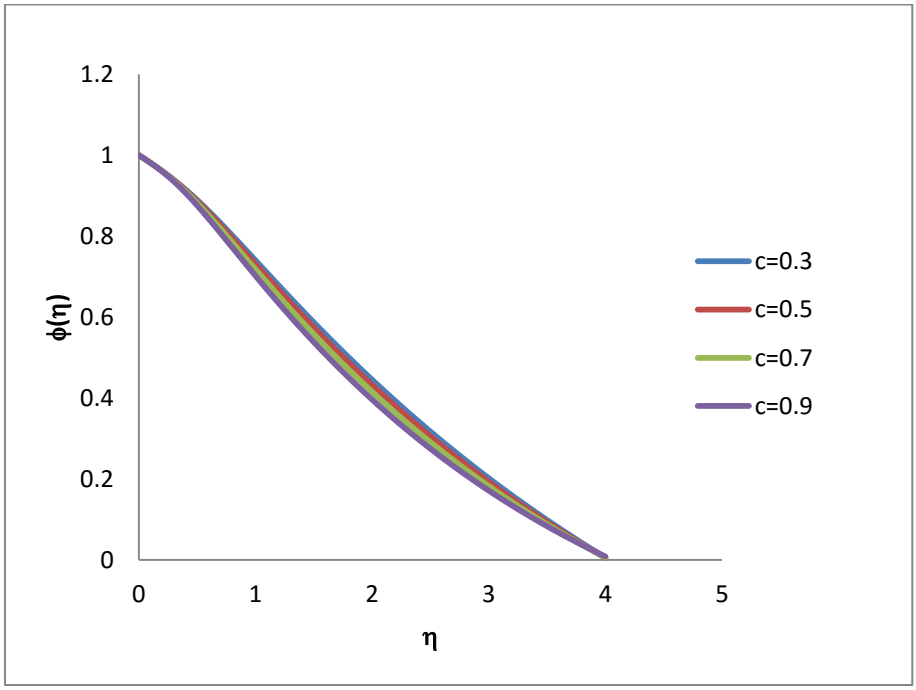

Fig 8.11 Effect of stretching ratio c on concentration $\phi(\eta)$; Pr=7.0; k=0.2; Sc=0.3; Sr=0.3; M = 1.0; N=0.5; β=0.5*

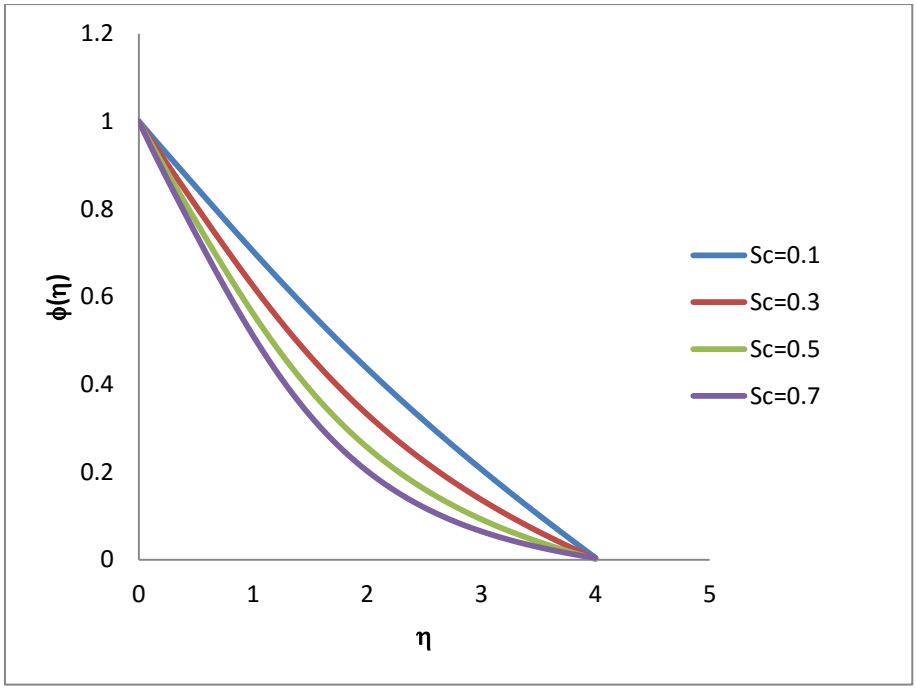

Fig 8.12 Effect of Sc on concentration $\phi(\eta)$; Pr=7.0; k=0.2; c=0.5; Sr=0.3; M = 1.0; N=0.5; β=0.5*

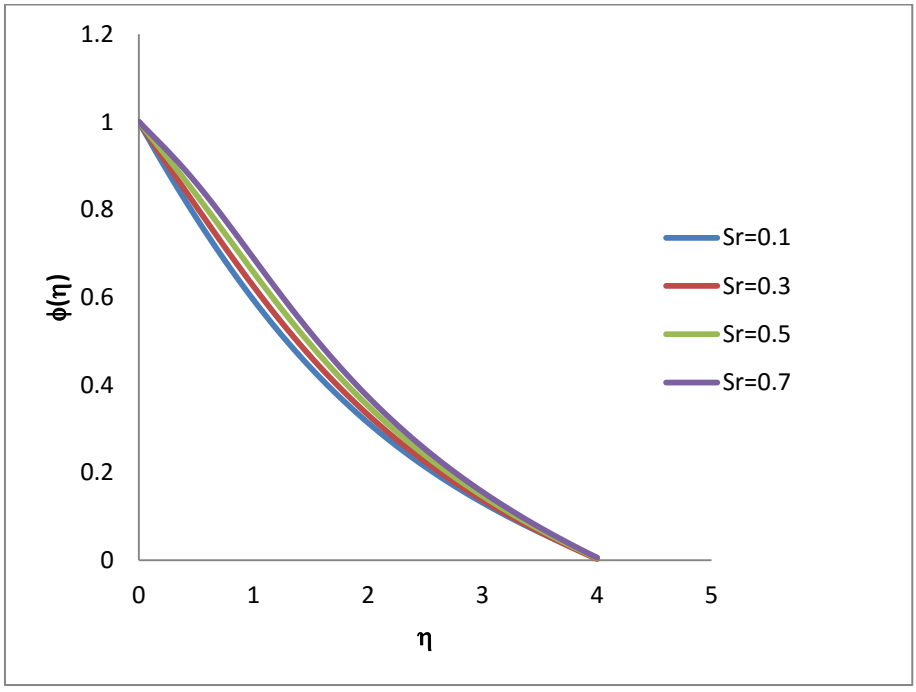

Fig 8.13 Effect of Sr on concentration $\phi(\eta)$; Pr=7.0; k=0.2; c=0.5; Sc=0.3; M = 1.0; N=0.5; β=0.5*

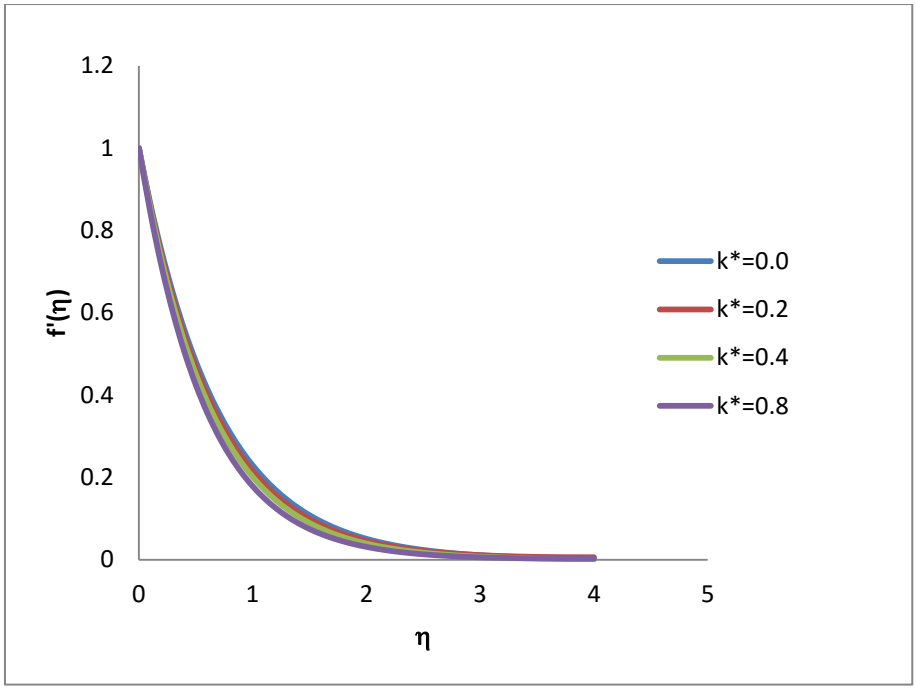

Fig 8.14 Effect of Porosity k^* on velocity $f'(\eta)$; Pr=7.0; Sc=0.3; c=0.5; Sr=0.3; M = 1.0; N=0.5; β=0.5

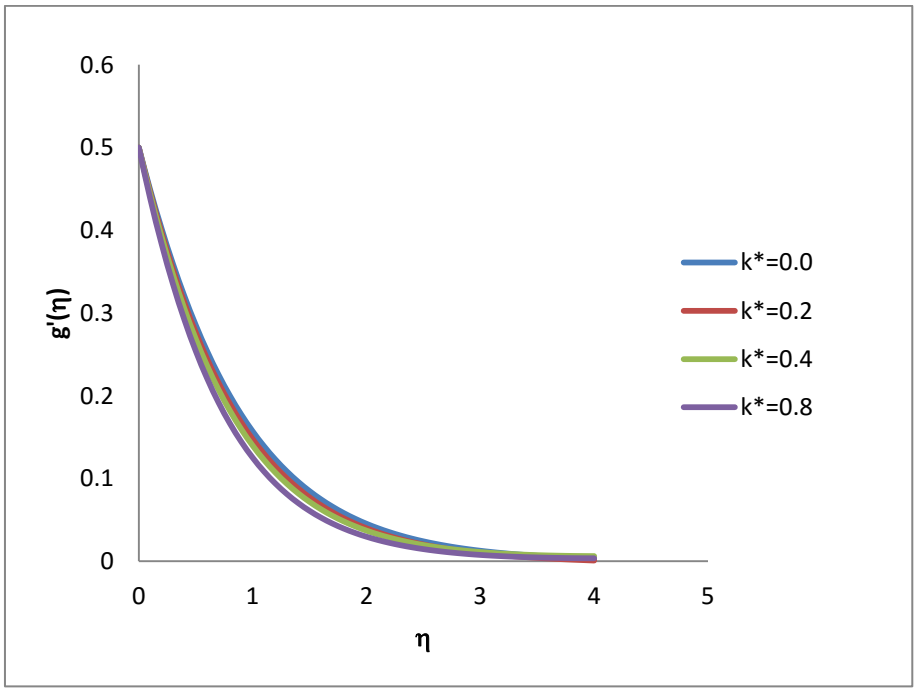

Fig 8.15 Effect of Porosity k^* on velocity $g'(\eta)$; Pr=7.0; Sc=0.3; c=0.5; Sr=0.3; M = 1.0; N=0.5; β=0.5

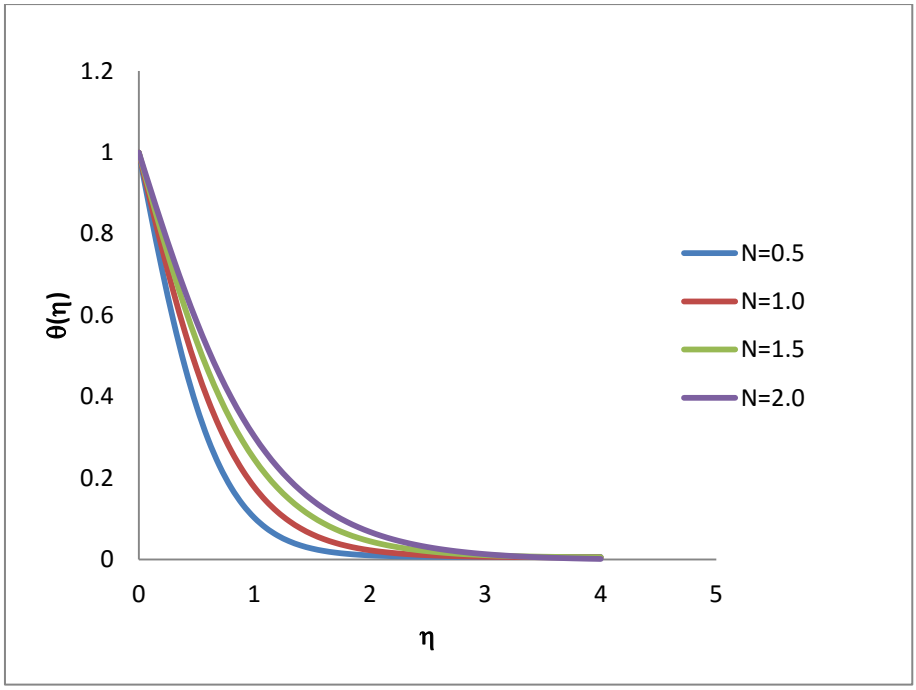

Fig 8.16 Effect of Radiation parameter N on temperature $\theta(\eta)$; Pr=7.0; Sc=0.3; c=0.5; Sr=0.3; M = 1.0; k=0.2; β=0.5*

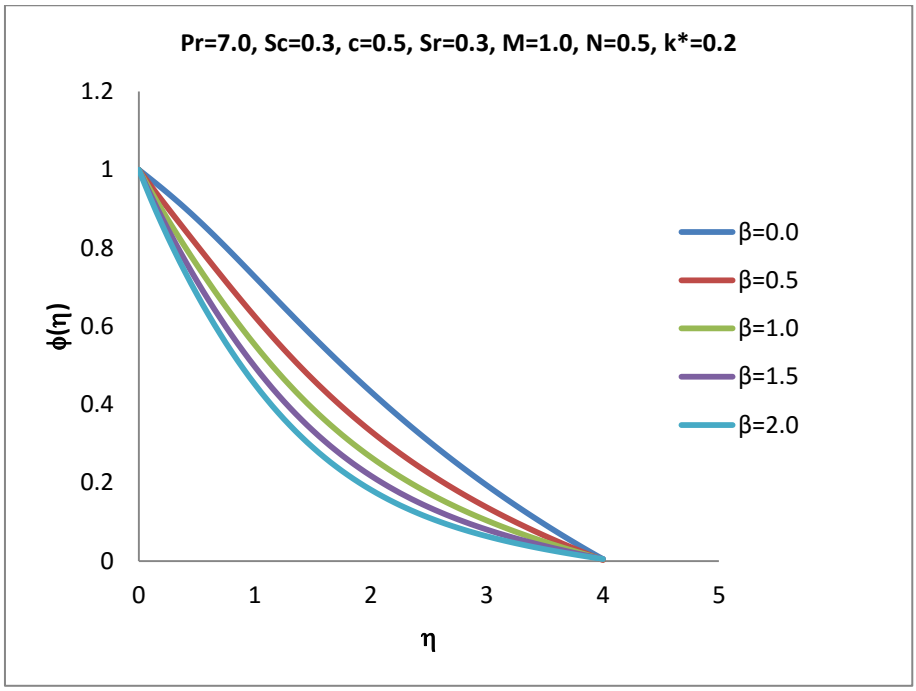

Fig 8.17 Effect of Chemical parameter β on concentration $\phi(\eta)$; Pr=7.0; Sc=0.3; c=0.5; Sr=0.3; M = 1.0; k=0.2; N=0.5*

M	N	β	c	f''(0)	θ'(0)	ϕ'(0)	g''(0)
0	0.5	0.5	0.5	-1.1355	-1.55821	-0.413	-0.46125
1	0.5	0.5	0.5	-1.51025	-1.47558	-0.405	-0.67591
2	0.5	0.5	0.5	-1.81106	-1.41756	-0.39988	-0.83968
3	0.5	0.5	0.5	-2.06866	-1.35756	-0.39799	-0.97695
1	0.5	0.5	0.5	-1.51025	-1.47558	-0.405	-0.67591
1	1	0.5	0.5	-1.51025	-1.19821	-0.425	-0.67591
1	1.5	0.5	0.5	-1.51025	-1.01982	-0.443	-0.67591
1	2	0.5	0.5	-1.51025	-0.89821	-0.4535	-0.67591
1	0.5	0	0.5	-1.51025	-1.47558	-0.23395	-0.67591
1	0.5	0.5	0.5	-1.51025	-1.47558	-0.405	-0.67591
1	0.5	1	0.5	-1.51025	-1.47558	-0.54093	-0.67591
1	0.5	1.5	0.5	-1.51025	-1.47558	-0.65595	-0.67591
1	0.5	0.5	0.3	-1.49313	-1.86134	-0.1883	-0.38677
1	0.5	0.5	0.5	-1.51025	-1.99892	-0.18798	-0.67591
1	0.5	0.5	0.7	-1.53593	-2.18613	-0.18758	-1.00798
1	0.5	0.5	0.9	-1.56876	-2.41861	-0.18718	-1.39428

Table 8.I Variation in $f''(0), -\theta'(0), \phi'(0)$ and $g''(0)$ for fluid at different non-dimensional parameters